Analysis of microbial diversity and community structure of rhizosphere soil of Cistanche salsa from different host plants

AiLing Liu
YuXia Li
QiQi Wang
XinRui Zhang
Jie Xiong
Yang Li
YanFei Sun (81711308@qq.com)
https://orcid.org/0000-0003-1947-9245
YongHui Lei

Research Article

Keywords: Cistanche salsa, High-throughput sequencing, Bacterial diversity, Fungal diversity, Rhizosphere soil

Posted Date: May 10th, 2022

DOI: https://doi.org/10.21203/rs.3.rs-1576900/v1

Abstract

Host plants influence *Cistanche* germination through root secretions, and plant rhizosphere bacteria influence host growth. Therefore, investigating the distribution of rhizosphere microorganisms in these host plants is crucial. Currently, good literature comparing the rhizosphere soil bacteria and fungi of different host plants of *Cistanche salsa* in the same habitat is lacking. High-throughput sequencing was used here to reveal the similarities and differences in the structural composition of the soil microbial community of *C. salsa* from six host plants (i.e., *Halocnemum*, *Atriplex*, *Kalidium*, *Tamarix*, *Anabasis*, and *Ceratoides*). We discovered that *Ceratoides*-parasitizing *C. salsa* had the highest diversity of rhizosphere bacterial communities, and *Anabasis*-parasitizing *C. salsa* had the highest diversity of rhizosphere fungal communities. *norank_f__norank_o__Actinomarinales* and *Aspergillus* were the most dominant bacterial and fungal genera, respectively. However, differences were noted in the contents of individual samples, which were attributable to the different host plants. RDA results also revealed that AP, HCO_3^-, pH, Ca^{2+}, SO_4^{2-}, and K^+ had a highly significant impact on the bacterial community structure ($P<0.01$), while pH and SO_4^{2-} had a significant impact on the fungal community structure ($P<0.05$). Moreover, bacteria are more vulnerable than fungi to soil physical and chemical indicators. Conclusively, differences were noted in the structure of rhizosphere bacterial and fungal communities of *C. salsa* parasitizing different plants in the same habit. A close correlation was observed between *C. salsa* and their host plants, soil microorganisms, and soil physical and chemical indicators. Our study findings can provide novel ideas for host plant selection and *C. salsa* cultivation.

1 Introduction

Cistanche salsa is a perennial parasitic plant belonging to the family *Orobanchaceae*. It has a high medicinal value and is known as the “desert ginseng”[1]. This genus includes five species: *C. deserticola*, *C. tubulosa*, *C. salsa*, *C. sinensis*, and *C. salsa va*.[2]. These species are mostly found in North Africa, the Arabian Peninsula, and Asia. In China, *Cistanche* plants are mainly distributed in Xinjiang, Gansu, Inner Mongolia, and Ningxia. Among these five species, *C. salsa* is commonly found in the desertification and salinization areas of XinJiang[3]. Host plants of *C. salsa* mainly include *Kalidium foliatum*, *Reaumuria soongorica*, *Nitraria tangutorum*, *Salsola passerine Bunge*, *Achnatherum splendens*, and other sand protection plants[4]. *C. salsa* has novel bud suckers at the base of its fleshy stem that infiltrate all areas of the host plant’s bast and xylem, causing the parasitized host root to cease functioning as a root system and instead serve as a channel for delivering nutrients to *Cistanche*[5]. Thus, cistanches and their host plants share a root. At present, numerous bioactive substances with crucial medicinal and edible values have been extracted from *C. salsa*[6]. These substances can improve memory, act as a laxative, and enhance kidney function. The market demand for *C. salsa* has increased dramatically because of its extremely high nutritional value, leading to overharvesting and a scarcity of *C. salsa* resources. Considering the substantial medicinal value and endangered status of *C. salsa* plants, protecting them is especially crucial.

Soil microorganisms are directly involved in processes such as plant nutrient extraction and soil nutrient cycling and are vital drivers of plant variety and production in terrestrial ecosystems. Rhizosphere microorganisms use plant inter-root secretions as a source of nutrients and interact with plants to influence their growth[7]. According to a previous study, rhizosphere microorganisms play a significant role in boosting the production of plant root secretions, chemical conversion and breakdown, and nutrient intake by the host, thereby increasing the parasitic plant’s parasitism rate[8]. Adequate study of rhizosphere soil microorganisms can help in improving plant nutrition and enhancing nutrient utilization[9]. Zheng et al. used 16S amplification sequencing to examine the microbial diversity of *C. salsa* soil in Abbey Salt Lake, thus laying the foundation for finding microbial molecular markers of *C. salsa* and promoting *C. salsa* growth, molecular breeding, and quality improvement research[10]. Consequently, investigating the microbial composition and diversity of *C. salsa* soil is crucial.

Host plants determine the entire growth and development of their parasitic plant. Host plant root exudates not only encourage parasitic plant seed germination but also boost the proliferation of host plant rhizosphere soil microbes[11]. Plant and soil types determine rhizosphere microbial diversity[12]; hence, effects on *Cistanche* growth and the rhizosphere microbial community are distinct for different host plants. Sun et al. compared the microbial community structure of three *Cistanche* ecotypes' rhizosphere soils and discovered that the communities of different ecotypes differed significantly[13]. Zhang et al. investigated echinacoside and acteoside concentrations in salt cistanches grown on various host plants and discovered that the host plants substantially affected the salt cistanche quality[14]. This indicated that the rhizosphere soil microbial communities of *Cistanche* parasitizing different host plants differ, and these differences may affect the germination and nutrient accumulation of *Cistanche*. However, no study has compared the rhizosphere microorganisms of different *Cistanche* host plants. To investigate the relationship between *C. salsa* and their host plants, soil microorganisms, and soil physical and chemical indicators, we collected six host plants of *C. salsa* (namely *Halocnemum*, *Atriplex*, *Kalidium*, *Tamarix*, *Anabasis*, and *Ceratoides*) found in saline areas of Qapqal County, Xinjiang and collected *C. salsa* from these plants. We performed physical and chemical indicator measurements as well as high-throughput sequencing on the rhizosphere soils surrounding the roots common to *C. salsa* and their host plants. To the best of our knowledge, this is the first study using high-throughput sequencing to investigate the diversity of bacteria and fungi in the rhizosphere soil of different *C. salsa* host plants in the same environment in Xinjiang.

2 Materials And Methods

2.1 Sampling and Processing

The sample collection sites are located in Qapqal County (43°50'26" N and 81°9'04"E) in Xinjiang, China. The local annual average temperature and precipitation were 9.1°C and 345 mm. The tested soil samples were obtained from the rhizospheres of different *C. salsa* host plants in saline-alkali land of Qapqal county. The six host plants were *Halocnemum* (YRCR1), *Atriplex* (YRCR2), *Kalidium* (YRCR3), *Tamarix* (YRCR4), *Anabasis* (YRCR5), and *Ceratoides* (YRCR6) (Fig. 1). Sterilized gloves and spades were used to collect the rhizosphere soil of the host plants, and the stone and plant debris were removed. The attached soil was then placed in individual germ-free bags and immediately placed in a 4°C incubator before being transported to the laboratory. The soil

sample was then split into two equal parts: one for determining the physical and chemical properties of the soil after air drying and the other for sequencing at − 80°C.

2.2 Physical and Chemical Properties of Soil

This study had six groups of test soil samples, and each sample was repeated three times. A naturally dried soil sample was mixed with distilled water at a ratio of 1:2.5 (W/V), 1:5 (W/V), and 1:5 (W/V) to form three suspensions, and then the soil suspensions were shaken for 20 min. pH of the 1:2.5 (W/V) soil suspension (with the electric potential method) was measured using a pH meter (Mettle-Toledo Instruments, Shanghai, China). The electrode method was used to determine conductivity (CO) of the 1:5 (W/V) soil suspension. The soil content of the eight major ions was determined using the 1:5 (W/V) soil suspension, with HCO^{3-} in the suspension titrated by double indicator neutralization, SO_4^{2-} by the EDTA volumetric method, Cl^- by silver nitrate titration, Ca^{2+} and Mg^{2+} by EDTA complex titration, and Na^+ and K^+ by the flame photometric method[15]. The potassium dichromate volumetric method–outside heating method was used to determine the organic matter (OM) content[16]. The Semimicro Macro Kjeldahl method and the indophenol blue spectrophotometric method were used to determine the total nitrogen (TN) and available nitrogen (AN) content of soil, respectively[17]. Bray I extraction–molybdenum antimony spectrophotometric and acid soluble molybdenum antimony colorimetric assays were used to measure the total phosphorus (TP) content. The amount of available phosphorus (AP) in the soil was determined using the molybdenum blue method after extracting AP with sodium bicarbonate. The ammonium acetate extraction flame photometry analysis was performed to analyze available potassium (AK) and total potassium (TK)[18]. $CHCl_3$ fumigation was used to measure soil microbial biomass carbon (MBC) and microbial biomass nitrogen (MBN)[19]. Glucose produced from a sucrose substrate was colorimetrically evaluated at 508 nm using a spectrophotometer to determine invertase (INV) activity[20]. Urease (UR) activity was determined by measuring the amount of ammonium released from a solution of urea (10%) and citrate buffer (pH 7) after 24 h of incubation at 37°C[21]. The conversion of disodium phenyl phosphate to phenol was used to measure phosphatase (PHA) activity[22]. Catalase (CAT) activity was determined by monitoring the decrease in H_2O_2 absorbance at 240 nm over 2 min and then applying an extinction coefficient of 40 $M^{-1}cm^{-1}$ for calculation[23]. Nitrate reductase (NR) activity was determined by incubating soil samples at 25°C for 24 h and controls at − 20°C. The released nitrates were extracted with 4 M KCl solution and colorimetrically measured at 520 nm[24].

2.3 DNA Extraction and PCR Amplification

Microbial community genomic DNA was extracted from *C. salsa* rhizosphere soil samples (0.5 g) using the EZNA® Soil DNA Kit (Omega Bio-tek, Norcross, GA, USA). The NanoDrop 2000 UV-Vis spectrophotometer (Thermo Scientific, Wilmington, USA) was used to determine DNA concentration and purity, and 1% agarose gel electrophoresis was used to ensure DNA quality and integrity. The bacterial 16S rRNA gene's hypervariable region V3–V4 was amplified with primer pairs: 515F (forward primer) (5'-GTGCCAGCMGCCGCGGTAA-3') and 806R (reverse primer) (5'-GGACTACHVGGGTWTCTAAT-3')[25–27]. The PCR system contained 4 μL of 5× FastPfu buffer solution, 2 μL of 2.5 mM dNTPs, 0.8 μL of 5 μM forward and reverse primers, 0.4 μL of DNA polymerase, 0.2 μL of BSA solution, and 10 ng template DNA, and finally, double-distilled H_2O was added to form a volume of 20 μL. The PCR was carried out on an ABI Gene Amp® 9700 PCR thermocycler (ABI, CA, USA), with an initial denaturation at 95°C for 3 min, followed by 27 cycles of denaturation at 95°C for 30 s, annealing at 55°C for 30 s, and extension at 72°C for 45 s, and a single extension at 72°C for 10 min, before finishing at 4°C. The fungal 5.8S rDNA gene was amplified with primer pairs: ITS1 (forward primer) (5'-CTTGGTCATTTAGAGGAAGTAA-3') and ITS2 (reverse primer) (5'-GCTGCGTTCTTCATCGATGC-3'). The PCR system included 2 μL of 10× FastPfu buffer solution, 2 μL of 2.5 mM dNTPs, 0.8 μL of 5 μM forward and reverse primers, 0.2 μL of rTaq of DNA polymerase, 0.2 μL of BSA solution, and 10 ng template DNA, and finally, double-distilled H_2O was added to form a volume of 20 μL. The PCR process consisted of an initial denaturation at 94℃ for 5 min, followed by 30 cycles of denaturation at 94℃ for 30 s, annealing at 55℃ for 30 s, extension at 72℃ for 1 min, and single extension at 72℃ for 7 min, before finishing at 4℃. The PCR thermocycler model was the same as that used for bacterial PCR.

2.4 Illumina MiSeq Sequencing

The PCR products were separated on 2% agarose gel electrophoresis, purified using the AxyPrep DNA Gel Extraction Kit (Axygen Biosciences, Union City, CA, USA) according to the manufacturer's instructions, and quantified using the QuantusTM Fluorometer (Promega, USA); each reaction was performed in triplicate[28]. Purified amplicons were pooled in equimolar proportions and paired-end sequenced on an Illumina MiSeq PE300 platform (Illumina, San Diego, USA) following the standard protocols of Meiji Biomedical Technology Co. Ltd. (Shanghai, China). The raw reads were uploaded to the NCBI Sequence Read Archive database (Accession Number: PRJNA764328).

2.5 Processing and Analyzing of Sequencing Data

Fastq version 0.20.0[29] was used to demultiplex and quality filter raw sequence files, and FLASH version 1.2.7[30] was used to merge them. The 300-bp reads were truncated at any site receiving an average quality score of < 20 over a 50-bp sliding window. The truncated reads shorter than 50 bp and the reads containing ambiguous characters were removed. Overlapping sequences greater than 10 bp were assembled according to their overlapped sequence, and those that could not be assembled were eliminated. The overlap region's maximum mismatch ratio was 0.2. The samples were distinguished on the basis of the barcode and primers, the sequence orientation was modified, the number of mismatches allowed by the barcode was set to 0, and the maximum number of primer mismatches was set to 2. With a 97% similarity cutoff, UPARSE version 7.1 was used to cluster operational taxonomic units (OTUs), and chimeric sequences were discovered and discarded[31, 32]. OTU-based taxonomy information can be used to conduct statistical analyses of the community structure at each classification level. RDP Classifier version 2.2 was used to assess the taxonomy of each OTU representative sequence against the 16S rRNA database (Silva 138) and the ITS database (Unite 8.0) with a confidence threshold of 0.7[33, 34].

2.6 Statistical analysis

Mothur v.1.30.2 was used to calculate alpha diversity, including the observed richness (Sobs), Chao1 estimator, ACE index, Shannon diversity index, and Simpson index, with a 97% similarity OTU[35]. The community ecology package was used to perform the principal coordinate analysis (PCoA), the Vegan 2.0

package was used to generate a PCoA figure, and Venn diagrams were generated using the Venn Diagram program[36], while redundancy analysis (RDA) and the heatmap figures were generated in Vegan 2.0 in R programming language[37]. SPSS Statistics v25.0 was used for analyzing data regarding soil physical and chemical parameters (IBM, USA). All values are presented as mean ± standard error (mean ± SE).

3 Results

3.1 Soil physicochemical properties

To explore how soil environmental factors affect soil bacterial communities, we measured soil pH, OM, TN, TP, TK, AN, AP, and AK (Table S1). At the same time, we tested CO and major ions of the soil, including Cl^-, SO_4^{2-}, Ca^{2+}, K^+, Mg^{2+}, Na^+, HCO_3^- (Table S2). Soil MBC and MBN content and CAT, UR, PHA, INV, NR activities were also measured (Table S3). The rhizosphere soil pH of different host plants fluctuated between 8.05 and 8.31, and significant differences in pH were noted between the samples($P < 0.05$). The OM and TN of YRCR4 and YRCR6 were significantly greater than those of the other samples ($P < 0.05$), and the OM and TN of YRCR2 were significantly lower ($P > 0.05$). YRCR4 had a considerably higher AN level than the other five samples ($P < 0.05$). The AN content of YRCR6 was immediately after that of YRCR4. The TP, TK, and AK content in YRCR6 was markedly higher than that in the other five samples ($P < 0.05$). The TP and TK content of YRCR4 was slightly lower than that of YRCR6. The AP content of YRCR5 was significantly higher than those of the other five samples, followed by YRCR6 and then YRCR4. The final results of the analysis showed that *C. salsa* parasitizing *Ceratoides* (YRCR6) and *Tamarix* (YRCR4) had higher OM, TN, TP, TK, AN, and AK content in the rhizosphere soil. The soil rhizosphere of *C. salsa* parasitizing Anabasis (YRCR5) had the greatest AP content. By analyzing the relationship between CO and salinity of the saturated leachate of soil, we collected six plants with rhizosphere soil salinity in the order of YRCR1, YRCR4, YRCR3, YRCR6, YRCR2, and YRCR5 from the highest to the lowest. Based on the content of each ion in the soil, the rhizosphere soil was found to be mainly dominated by sulfate, sodium, chloride, and calcium salts. The analysis of measured ions showed the same trend for Na^+ and Cl^- content in each sample and for CO, with significant differences observed among all samples ($P < 0.05$). The contents of other ions exhibited variable trends among the samples, but were the lowest in YRCR5. The enzyme activity assay showed high CAT, UR, PHA, and INV activities in YRCR6.

3.2 Alpha diversity analysis of sequencing data

After read-quality filtering, Illumina-based analysis of the hypervariable V3-V4 region of the bacterial 16S rRNA gene yielded 1207863 high-quality reads, and the analysis of the ITS1 region of the fungi produced 1230526 high-quality reads. Each sample included an average of 67,104 and 68,363 bacterial and fungal reads, respectively. The average read length for bacteria was 253 bases and for fungi was 245 bases. The rhizosphere bacterial community contained 45 phyla, 121 classes, 292 orders, 491 families, 854 genera, 1451 species, and 4566 OTUs, while the rhizosphere fungal community contained 9 phyla, 29 classes, 60 orders, 139 families, 247 genera, 368 species, and 819 OTUs based on the minimum sample sequence. A total of 4566 OTUs for bacterial diversity and 819 OTUs for fungal diversity were generated for each sample based on 97% similarity. The Shannon rarefaction curves of bacteria and fungi tended to be smooth, reflecting the availability of sufficient sequencing data (Fig. 2). The coverage valuation of both bacteria and fungi reached 99%, indicating that only a very few sequences were not detected in the samples (Table 1). Therefore, the alpha diversity index of bacteria and fungi in the sequenced samples represent the abundance and diversity of bacteria and fungi. Our analysis showed that the highest bacterial diversity was found in *C.salsa* parasitizing *Ceratoides* (YRCR6) and the lowest bacterial diversity was found in *C. salsa* parasitizing *Anabasis* (YRCR5). No remarkable differences ($P > 0.05$) were noted in bacterial diversity among the four samples YRCR4, YRCR2, YRCR3, and YRCR1. The highest fungal community diversity was found in *C. salsa* parasitizing *Anabasis* (YRCR5), which was significantly different from that of *C. salsa* parasitizing *Tamarix* (YRCR4) and *Ceratoides* (YRCR6) ($P < 0.05$). In addition, no significant differences in fungal community diversity were noted among the other samples ($P > 0.05$). The abundance of the bacterial community of *C. salsa* parasitizing *Kalidium* (YRCR3) was significantly lower than that of other samples, according to the Chao 1 index and ACE index analyses, and no statistically significant difference was observed in bacterial community abundance across the remaining five samples. *C. salsa* parasitizing *Ceratoides* (YRCR6) had the highest fungal community abundance, followed by YRCR2. Although no significant difference in abundances was noted between YRCR6 and YRCR2 ($P > 0.05$); the abundances in these samples were significantly higher than those in the other samples. In the remaining four samples, no significant differences were noted in the abundance of fungal communities ($P > 0.05$). Overall, the bacterial community diversity and abundance was maximum in the rhizosphere soils of *C. salsa* parasitizing *Ceratoides* (YRCR6). The rhizosphere soil of *C. salsa* parasitizing *Anabasis* (YRCR5) had the most diversity of fungal communities, whereas that of *C. salsa* parasitizing *Ceratoides* (YRCR6) had the highest abundance.

Table 1
Alpha diversity indices of bacteria and fungi in rhizosphere soil of *C.salsa* with different host plant.

sample ID	OUT(97%)		Sobs		Chao1		Ace		Shannon		Simpson		Coverage(%)	
	Bacteria	Fungi	Bacteria	Fungi	Bacteria	Fungi	Bacteria	Fungi	Bacteria	Fungi	Bacteria	Fungi	Bacteria	Fu
YRCR1	3061	255	2385.00 ± 81.07 abc	155.67 ± 9.81 b	2944.14 ± 50.76 a	164.62 ± 8.73 b	2929.52 ± 76.93 a	163.32 ± 8.86 b	5.90 ± 0.15 b	3.38 ± 0.59 a	0.01 ± 0.00 b	0.10 ± 0.08 ab	99.10	99.
YRCR2	3092	336	2434.67 ± 34.27 ab	201.67 ± 29.84 a	2940.99 ± 86.16 a	207.79 ± 31.86 a	2938.21 ± 70.65 a	205.88 ± 29.75 a	5.89 ± 0.04 b	3.41 ± 0.50 a	0.02 ± 0.01 b	0.10 ± 0.07 ab	99.12	99.
YRCR3	2658	248	2022.00 ± 70.93 d	152.00 ± 7.81 b	2530.35 ± 44.68 b	158.44 ± 13.62 b	2539.09 ± 47.38 b	159.39 ± 14.36 b	5.68 ± 0.11 c	2.90 ± 0.56 ab	0.02 ± 0.01 b	0.18 ± 0.11 ab	99.19	99.
YRCR4	2979	277	2311.00 ± 67.67 bc	149.33 ± 10.12 b	2869.09 ± 109.74 a	161.97 ± 13.52 b	2836.79 ± 69.22 a	157.57 ± 12.28 b	5.79 ± 0.11 bc	2.49 ± 0.47 b	0.02 ± 0.01 b	0.23 ± 0.08 a	99.11	99.
YRCR5	2973	279	2278.00 ± 108.02 c	169.00 ± 7.00 b	2861.53 ± 133.08 a	173.46 ± 3.83 b	2854.90 ± 118.50 a	173.11 ± 5.96 b	5.37 ± 0.14 d	3.56 ± 0.07 a	0.01 ± 0.01 a	0.07 ± 0.00 b	99.13	99.
YRCR6	3055	309	2473.00 ± 38.59 a	210.00 ± 6.24 a	2964.40 ± 26.58 a	225.72 ± 6.34 a	2926.02 ± 34.53 a	226.36 ± 6.49 a	6.22 ± 0.05 a	2.44 ± 0.05 b	0.01 ± 0.00 c	0.17 ± 0.02 ab	99.17	99.

Sobs indices was used to evaluate the number of observable OTUs; Chao 1 and ACE indices were used to evaluate species richness; Shannon and Simpson indices were used to evaluate species diversity; Data was shown by the average of three replicates and their standard deviation. Different letters following aft the data indicated significant differences (P□0.05) based on Kruskal-Wallis test. YRCR1, *C.salsa* parasitic on *Halocnemum Bieb*; YRCR2, *C.salsa* parasitic on *Atriplex L.*; YRCR3, *C.salsa* parasitic on *Kalidium Moq*; YRCR4, *C.salsa* parasitic on *Tamarix L.*; YRCR5, *C.salsa* parasitic on *Nitraria L.*; YRCR6, *C.salsa* parasit on *Ceratoides*.

3.3 Bacterial community analysis

High-throughput sequencing revealed the diversity of bacterial communities in different samples. At the phylum level, 37 phyla were identified, and Fig. 3 shows the relative abundance of the top 13 phyla (relative abundance > 1%). *Actinobacteriota*, *Proteobacteria*, *Chloroflexi*, *Gemmatimonadota*, *Bacteroidota*, *Crenarchaeota*, *Planctomycetota*, *Halobacterota*, *Acidobacteriota*, *Firmicutes*, *Thermoplasmatota*, *Patescibacteria*, and *Myxococcota* were detected in the rhizosphere soil of the six host plants. However, their relative abundance varied in different host plant soils. The most abundant phylum in the six samples was *Actinobacteriota*, which accounted for 32.2% of all samples (Fig. 3. a), and its abundance in the soil samples of each host plant ranged from high to low: YCRC5 (37.45%), YCRC2 (33.26%), YCRC3 (33.01%), YCRC4 (32.72%), YCRC1 (28.26%), and YRCR6 (28.12%) (Fig. 3. b). *Proteobacteria* was the second abundant phylum, accounting for 18.89% of all the samples, and its abundance in the soil samples of each host plant was YCRC1 (20.85%), YCRC4 (20.31%), YCRC3 (20.30%), YCRC2 (18.68%), YCRC5 (16.67%), and YCRC6 (16.65%) in the descending order. *Chloroflexi* accounted for 9.68% of all sample populations, with its relative abundance being greater in YCRC6 than in the other samples. *Gemmatimonadota* accounted for 9.41% of all sample populations, with its relative abundance being higher in YCRC3 than in the other five samples. *Bacteroidota* accounted for 5.31% of all the samples, with its relative abundance being higher in YCRC1 than in the other samples. *Crenarchaeota* accounted for 5.09% of all samples and had the highest relative abundance in YCRC5. *Planctomycetota* (4.50%), *Halobacterota* (3.10%), *Acidobacteriota* (2.14%), *Firmicutes* (2.07%), *Thermoplasmatota* (2.00%), *Patescibacteria* (1.02%), and *Myxococcota* (1.03%) were the phyla with relatively low abundance among all samples.

A total of 854 genera were identified from all rhizosphere soil samples, further analysis revealed 456 common genera in the six samples (Fig. 4. a). The top 10 genera in the order of relative abundance (relative abundance > 1%) were *norank_f__norank_o__Actinomarinales* (14.11%), *norank_f__Geminicoccaceae* (4.91%), *norank_f__norank_o__norank_c__BD211_terrestrial_group* (4.19%), *norank_f__Nitrososphaeraceae* (3.01%), *norank_f__norank_o__norank_c__Alphaproteobacteria* (2.25%), *norank_f__Euzebyaceae* (2.22%), *norank_f__norank_o__norank_c__PAUC43f_marine_benthic_group* (1.95%), *norank_f__Rhodothermaceae* (1.91%), *norank_f__67 − 14* (1.83%), and *Candidatus_Nitrososphaera* (1.80%) (Figure S2. a). We then analyzed the variability of these genera among the six samples at the genus level (Fig. 5.a), remarkable differences were observed in the relative abundance of 10 dominating genera among the six *C. salsa* host plant samples ($P < 0.05$). Among them, *norank_f__norank_o__norank_c__Alphaproteobacteria* and *norank_f__Euzebyaceae* showed extremely significant differences ($P < 0.01$) in the relative abundance among all samples. *Norank_f__norank_o__Actinomarinales* and *norank_f__Geminicoccaceae* were mainly found in YCRC5. *Norank_f__norank_o__norank_c__BD2-11_terrestrial_group*, *norank_f__norank_o__norank_c__PAUC43f_marine_benthic_group*, and *norank_f__Nitriliruptoraceae* were mainly present in YCRC3. *Norank_f__norank_o__norank_c__Alphaproteobacteria* and *norank_f__Rhodothermaceae* were mainly detected in YCRC4. *Norank_f__Euzebyaceae* and *Candidatus_Nitrososphaera* mainly existed in YCRC6. *Norank_f__67 − 14* was mainly detected in YCRC3 and YCRC6.

3.4 Fungal community analysis

The composition of fungal communities in all samples was simpler than that of bacterial communities. Nine fungal phyla were found in all samples, with five phyla having a relative abundance of > 1%: *Ascomycota*, *Basidiomycota*, *unclassifed fied_k__fungi*, *Mortierellomycota*, and *Chytridiomycota* (Fig. 3. c). Among all the phyla, *Ascomycota* was the main dominant phylum and accounted for 85.17% of all the fungal phyla. The secondary dominant phyla included *Basidiomycota*, *unclassified_k__Fungi*, *Mortierellomycota*, and *Chytridiomycota*, which accounted for 7.85%, 3.16%, 2.55%, and 1.05% of all fungal phyla, respectively. However, the predominance of other phyla in each independent sample, except *Ascomycota*, was different. The relative abundance of *Mortierellomycota* was higher in YCRC1 and YCRC5 than in the other phyla, that of *unclassified_k__Fungi* was higher in YCRC2 than in the other phyla, and that of *unclassified_k__Fungi* was higher in YCRC4 than in the other phyla (Fig. 3. d).

In addition, we analyzed the fungal community structure at the genus level and discovered 247 fungal genera, further analysis revealed 35 common genera in the six samples (Fig. 4. b). Community barplot analysis showed the 23 genera with relative abundances of > 1%. The proportion of fungi in the top 15 genera with a relative abundance ranging from the highest to lowest were *Aspergillus* (16.94%), *Penicillium* (8.71%), *Chaetomium* (7.42%), *Sporormia* (7.05%), *Wallemia* (5.54%), *unclassified_p __Ascomycota* (3.90%), *Talaromyces* (3.70%), *Alternaria* (3.63%), *Pseudogymnoascus* (3.33%), *unclassified_k__Fungi* (3.16%), *Neocamarosporium* (2.61%), *Mortierella* (2.53%), *Engyodontium* (2.52%), *unclassified_c__Sordariomycetes* (2.38%), and *Monosporascus* (2.15%) (Figure S2. b). Next, we analyzed the variability of these genera among the six samples at the genus level (Fig. 5.b). Significant differences ($P < 0.05$) were noted across all 10 genera in all samples. *Aspergillus* differed extremely significantly ($P < 0.01$) among the six samples. *Aspergillus* and *Pseudogymnoascus* were mainly present in YCRC4. *Wallemia* was mainly found in YCRC6. *Penicillium* was mainly present in YCRC2 and YCRC6. *unclassified_p__Ascomycota* was mainly found in YCRC1. *Alternaria* and *unclassified_k__Fungi* were mainly observed in YCRC2. *Talaromyces* was almost exclusively present in YRCR5, and *Mortierella* was mainly detected in YCRC5. *Engyodontium* was mainly found in YCRC3.

3.5 Comparison of bacterial and fungal communities of different samples

Bacterial and fungal communities in all soil samples were compared separately at the OTU level by using PCoA based on the Bray–Curtis matrix algorithm and hierarchical clustering to identify parallels or variations in community composition between groups of samples. The first PCoA axis (PCoA1) explains 35.99% of the overall variation in the bacterial community, while the second PCoA axis (PCoA2) explains 22.36% of the entire variation in the bacterial community (Fig. 6. b). Among the six soil samples, three replicates clustered together within each sample group showed good reproducibility, and a good separation was noted between each grouped sample. Meanwhile, the principal component analysis diagram clearly showed that YCRC1, YCRC3, and YCRC4 are similar in bacterial community composition, and YCRC2 and YCRC5 are similar in bacterial community composition. This conclusion corresponds with that of the sample hierarchical cluster analysis plot (Fig. 6. a). Adonis was used to analyze the average difference and significance between the six samples. The results showed that the R^2 value ($R^2 = 0.8528$) was greater than 0 and tended to 1, suggesting that the differences between the sample groups were greater than those within the sample groups. A P value of < 0.05 ($P = 0.001$) indicated significant differences between sample groups.

Similarly, the fungal communities were subjected to PCoA. PCoA1 and PCoA2 alone explained 23% and 18.16% of the variance, respectively (Fig. 6. c). Except for YCRC1, YCRC3 and YCRC4 exhibited high similarity, whereas YCRC6 exhibited a low similarity with the other five samples, which is consistent with the sample level clustering result (Fig. 6. d). Adonis analysis results showed that the R^2 value was 0.7653, suggesting that the difference between the total samples was higher than that within the group. A P value of < 0.05 ($P = 0.001$) indicated that the difference between the samples was significant.

3.6 Relationship between bacterial and fungal community structures and soil properties

RDA revealed the influence of many environmental conditions on soil microbial communities, as well as the correlation between them. RDA was performed for the top 10 bacterial genera and soil physicochemical properties. The results showed that the first RDA axis accounted for 62.05% of the total variance and the second axis accounted for 12.74% of the total variance, with a total variance of 74.79% for both axes (Fig. 7. a). At a 0.05 significance level, SO_4^{2-} had a positive and significant correlation with *norank_f__norank_o__norank_c__BD-211_terrestrial_group*, *norank_f__norank_o__norank_c__PAUC43f_marine_benthic_group*, and *norank_f__Rhodothermaceae*. Ca^{2+} exhibited a positive and significant correlation with *norank_f__Rhodothermaceae*, whereas it exhibited a considerable negative relationship with *norank_f__Geminicoccaceae* and *norank_f__Nitrososphaeraceae*. pH and K^+ had significant positive correlations with *norank_f__Euzebyaceae* and negative correlations with *norank_f__norank_o__Actinomarinales*. In addition, like OM, K^+ had significant positive correlations with *norank_f__67 − 14*, *norank_f__norank_o__norank_c__Alphaproteobacteria*, and *Candidatus_Nitrososphaera*. HCO_3^- was significantly and negatively correlated with *norank_f__Nitrososphaeraceae*, *norank_f__norank_o__norank_c__PAUC43f_marine_benthic_group*, and *norank_f__norank_o__norank_c__BD-211_terrestrial_group*, whereas it was significantly and positively correlated with *norank_f__norank_o__norank_c__Alphaproteobacteria* (Figure S1.a). Among the environmental factors analyzed for RDA, SO_4^{2-}, AP, and HCO_3^- had the greatest impact on the rhizosphere soil bacterial community structure ($P = 0.003$), followed by pH ($P = 0.006$), Ca^{2+} ($P = 0.024$), and K^+ ($P = 0.020$). OM ($P = 0.147$) had the least effect on the bacterial community structure (Table S1).

Similarly, RDA was performed for the top 10 fungal genera and soil physicochemical properties, the results showed that the first RDA axis accounted for 27.55% of the total variance and the second axis accounted for 16.58% of the total variance, with a total variance of 44.13% for both axes (Fig. 7. b). At a 0.05 significance level, AP was markedly positively connected with *Aspergillus* and *Talaromyces* and negatively linked with *Pseudogymnoascus* and *unclassified_p__Ascomycota*. SO_4^{2-} was significantly positively linked with *unclassified_p__Ascomycota* and significantly negatively linked with *Alternaria*, *Wallemia*, and *Penicillium*. On the contrary, HCO_3^- was significantly positively correlated with *Wallemia* and *Penicillium*. pH showed a significant negative correlation with *Aspergillus*. K^+ was significantly and positively connected with *Chaetomium* (Figure S1.b). Among these environmental factors, pH had the greatest effect on the rhizosphere soil fungal community structure ($P = 0.001$), followed by SO_4^{2-} ($P = 0.014$). K^+ ($P = 0.078$), HCO_3^- ($P = 0.085$), OM ($P = 0.150$), Ca_2^+ ($P = 0.163$), and AP ($P = 0.174$) all had a very small effect (Table S4).

4 Discussion

In this study, high-throughput sequencing was used to explore the diversity and abundance of bacteria and fungi in the rhizosphere soil of *C. salsa* from various host plants. We also compared the differences in bacterial and fungal community structures in the *C. salsa* rhizosphere soil and revealed the relationship between bacteria and fungi in soil samples and soil properties. The abundance of soil bacteria and fungi, as well as the diversity of bacteria, was higher in the rhizosphere soil of *C. salsa* parasitizing *Ceratoides* (YRCR6) than in the other five samples. Although the highest fungal diversity was observed in the rhizosphere soil of *C. salsa* parasitizing *Anabasis* (YRCR5), Simpson's index showed no significant difference between YRCR5 and YRCR6. This may be attributed to the high resiliency and unique adaptation mechanism of *Ceratoide*s to harsh environments, such as its capacity to fully absorb soil nutrients while adapting to saline conditions and preserving the stability of its rhizosphere microbial community. Soil physical and chemical properties are intimately related to the soil microbial community structure, and soil properties can significantly improve the structural composition and species richness of microbial communities [38, 39]. Soil enzymes are mostly synthesized by soil microorganisms, plants, and animals, and these enzymes play a role in the conversion, synthesis, and breakdown of OM as well as the oxidation and reduction of inorganic substances in soil[40, 41]. Our results showed that the enzyme activity of YRCR6 was higher than that of the other samples, with higher MBC and MBN content. Such results could indicate that the soil microenvironment of *C. salsa* parasitizing *Ceratoides* (YRCR6) was more active, which corresponds with the high-through sequencing results. pH is an important factor affecting the microbial community structure, and studies have found that higher the pH, lower the structural diversity of bacterial and fungal communities[42]. However, our findings differ slightly from those of previous studies. Our data showed that the pH of YRCR4 was considerably lower than that of YRCR6 ($P < 0.05$), while the alpha diversity index of bacteria was also remarkedly lower than that of YRCR6. This might be attributable to the fact that YRCR4 is more salinized than YRCR6, which caused changes in other physical and chemical variables of the soil and thus influenced the bacterial community diversity in YRCR4. As soil salinity increases, soils experience high pH and alkalinity, lower soil microbial populations, changes in the community structure, and reduced diversity[43]. We found that the fungal diversity of YRCR4 was not consistent with pH variation, which was anomalous to other samples. The reason may be high soil salinization and high soil pH that limit fungal growth[44]. This may also be a reason for the lower diversity of fungal communities than of bacterial communities. OM influences soil microbial community diversity and increasing OM concentration enhances this diversity [45]. The OM content of YRCR4 and YRCR6 was significantly greater than that of the remain samples, and the bacterial diversity of YRCR6 was also higher than that of the other samples. The diversity of YRCR4 was significantly lower than that of YRCR6 may be due to the other factors and not due the OM content of YRCR4 and YRCR6, which showed no significant difference. Contrary to bacterial diversity, YRCR4 and YRCR6 exhibited lower fungal diversity than the other samples. This may be because fungal diversity in soil decreases with increasing OM content at a small local scale[46, 47]. The soil nitrogen source promotes OM decomposition by microorganisms and increases bacterial diversity[48], but it also suppresses the fungal population[49]; the fungal population decreases as the AN content increases [50]. Our data showed higher AN content in YRCR4 and YRCR6 than in the other samples, and YRCR6 had the highest bacterial diversity and lower fungal diversity than several other samples, which showed the same results as the previous study. The increase in phosphorus and potassium content increases microbial biomass and diversifies bacterial communities[51], while phosphorus content significantly affects the abundance of soil fungal communities[52]. In our study, YRCR6 had significantly higher P and K content than other samples, and YRCR6 had higher abundance of bacterial and fungal communities than other samples. Conclusively, soil physical and chemistry markedly influences soil microorganisms, and an inextricable relationship exists between host plants and soil microorganisms.

Our sequencing results showed that 854 bacterial genera were found in the rhizosphere soil samples of the six host plants, of which *norank_f__norank_o__Actinomarinales* showed the largest relative abundance (14.11%). This is consistent with the results of other studies suggesting that the dominance of *Actinobacteriota* increases with increasing soil salinity[53]. Sun et al. also concluded that the soil microbial communities for *C. salsa* are mostly tolerant to drought, salt, and alkali and are more resistant to stress[13]. *Actinobacteriota* happens to exhibit this function. Moreover, it participates in soil nutrient cycling and forms bioactive secondary metabolites[54]. Therefore, *Actinobacteriota* has an osmoprotective effect on cistanches and increases the salinity resistance of *C. salsa*. Our sample collection sites were in saline areas, which may also account for the high proportion of *norank_f__norank_o__Actinomarinales*. However, this proportion differed among the samples, which may have resulted from differences in host plants, because even within the same microbial pool, plants can actively recruit plant-associated microorganisms from the soil to build specific microbial communities[53]. RDA also showed that *norank_f__norank_o__Actinomarinales* had significant negative correlations with pH and K^+ ($P < 0.05$) but no significant correlations with other indicators, which agrees with the results of the comparative analysis of species differences among the samples. Relative to *norank_f__norank_o__Actinomarinales*, the other genera are all represented by a lower proportion of *norank_f__Geminicoccaceae*, (4.91%), *norank_f__norank_o__norank_c__BD211_ terrestrial_group* (4.19%), *norank_f__Nitrososphaeraceae* (3.01%), *norank_f__norank_o__norank_c__Alphaproteobacteria* (2.25%), and *norank_f__ Euzebyaceae* (2.22%), which may be due to soil salinization affecting the rhizosphere soil quality and microenvironment, thereby influencing soil microbial colonization and thus changing the soil microbial community occupancy. Dominant bacteria are crucial determinants of microbial community balance, which affects the structural composition of these communities. We found that Ascomycota is the dominant fungal phylum, and most of Ascomycota are saprophytic[55], which are able to decompose difficult-to-degrade substances such as lignin and keratin, and thus improve soil quality. The second dominant fungal phylum is Basidiomycota; the results are identical to those of SuiXin[56] and Gaoweiwei[57]. At the genus level, *Aspergillus* is the dominant fungal genus with the role of decomposing cellulose and removing heavy metals from the soil[58]. Such results are closely related to the fact that the samples were collected from salinized soils, where saline plants recruit specific microorganisms to serve them and help them decompose and absorb salt ions from the soil, thus allowing *Cistanche* to grow better. *Penicillium* is the second dominant genus, which has better antibacterial activity and can protect *Cistanche* and its host plants from pathogenic bacteria to some extent[59]. RDA showed that *Aspergillus* and *Talaromyces* were markedly positively connected with AP, whereas *Pseudogymnoascus* and *unclassified_p__Ascomycota* were negatively correlated. SO_4^{2-} was significantly positively correlated with *unclassified_p__Ascomycota* and significantly negatively correlated with *Alternaria*, *Wallemia*, and *Penicillium*, indicating that fungal genera differ in their ability to adapt to their environment and that changes in environmental factors can cause changes in the fungal community structure.

5 Conclusion

We here used high-throughput sequencing to analyze bacterial and fungal diversity in the rhizosphere soil of different *C. salsa* host plants. This is the first study analyzing the characteristics of rhizosphere microorganisms of different *C. salsa* host plants using a high-throughput method.

Our results showed that among the six *C. salsa* host plants, the bacterial diversity of the rhizosphere soil of *C. salsa* parasitizing *Ceratoides* was significantly higher than that of the other samples, and the fungal diversity of *C. salsa* parasitizing *Anabasis* was higher than that of the other samples. The most dominant bacterial genus in the six samples was *Norank_f__norank_o__Actinomarinales*, and the most dominant fungal genus was *Aspergillus*. Meanwhile, the results of our analysis showed that bacterial and fungal community structures differed among the different host plants, which were not only related to rhizosphere soil physical and chemical indicators but also closely associated with the *C. salsa* and their host plant root secretion. We believe a complex relationship exists between *C. salsa*, their host plants, rhizosphere microorganisms, and soil physical and chemical indicators, which interact and influence each other. Our research provides novel ideas for the artificial selection of *C. salsa* host plants, development of salt-tolerant fungicides, and management of the saline ecological environment.

Declarations

Data Availability

The date of high through-put sequencing in this project have been deposited in the Sequence Read Archive (SRA) of the National Center for Biotechnology Information (NCBI) under the accession number PRJNA764328(https://www.ncbi.nlm.nih.gov/search/all/?term=PRJNA7643280)

Acknowledgements

The authors would like to thank all the reviewers who participated in the review, as well as MJEditor (www.mjeditor.com) for providing English editing services during the preparation of this manuscript.

Funding

The work was financially supported by the national natural science foundation of China (project number: 31460070).

Author information

Affiliations

College of life Science / Xinjiang Production and Construction Corps Key Laboratory of Oasis Town and Mountain-basin System Ecology, North 4 Street, College of life Science, Shihezi University, Shihezi, 832003, China

YanFei Sun, Ailing Liu, YuXia Li, QiQi Wang, XinRiu Zhang, Jie Xiong, Yang Li

College of Agriculture, Shihezi University, Shihezi, 832003, China.

YongHui Lei

Contributions

LAL designed and performed the experiments, analyzed the data, and drafted the manuscript. LYX helped analyzing the data, revised and refined the manuscript. WQQ and ZXR performed sample collection and analyzed part of the data. LY participated in analyzing the dates and drafting the manuscript. XJ performed soil chemical property analysis, DNA extraction and PCR amplification. SYF and LYH designed and performed the experiments and analyzed data. All authors read and approved the final manuscript.

Corresponding author

Correspondence to YanFei Sun and YongHui Lei.

Declaration of competing interest

All of the authors declare that they have no known competing financial interests or personal relationships that could have appeared to influence the work reported in this paper.

References

1. Wu CJ, Chien MY, Lin NH, Lin YC, Chen WY, Chen CH, Tzen JTC (2019) Echinacoside Isolated from Cistanche tubulosa Putatively Stimulates Growth Hormone Secretion via Activation of the Ghrelin Receptor. Molecules (Basel, Switzerland) 24. doi: 10.3390/molecules24040720
2. Yang K, Yang QH, Yang SQ, L SQ (2011) The research progress of cistanche hoffing.et link. J Inner Mongolia Med Univ 33(05):434–437. https://doi.org/10.16343/j.cnki.issn.2095-512x.2011.05.006
3. Zheng S, Jiang X, Wu L, Wang Z, Huang L (2014) Chemical and Genetic Discrimination of Cistanches Herba Based on UPLC-QTOF/MS and DNA Barcoding. PLoS ONE 9:e98061. https://doi.org/10.1371/journal.pone.0098061

4. Wen D (2008) Studies on the Classification and the Host Plants of Chinese Cistanche Hoffmg.et Link. Inner Mongolia University,China
5. Chen JY, Chen XL, Guo NN, Ma WB, Da QJ, Zhang HX (2016) Difference of parasitic form of Cynomorium songaricum and Cistanche deserticola. Guihaia36(11):1312–1317 + 1343. ISSN: 1000–3142
6. Trampetti F, Pereira C, Rodrigues MJ, Celaj O et al (2019) Exploring the halophyte Cistanche phelypaea (L.) Cout as a source of health promoting products: In vitro antioxidant and enzyme inhibitory properties, metabolomic profile and computational studies. J Pharm Biomed Anal 165:119–128. https://doi.org/10.1016/j.jpba.2018.11.053
7. Bulgarelli D, Schlaeppi K, Spaepen S, Themaat EVL, Schulze-Lefert P (2012) Structure and functions of the bacterial microbiota of plants. Annu Rev Plant Biol 64:807–838. https://doi.org/10.1146/annurev-arplant-050312-120106
8. Akiyama K, Hayashi (2006) Strigolactones: chemical signals for fungal symbionts and parasitic weeds in plant roots. ANN BOT 97:925–931. https://doi.org/10.1093/aob/mcl063
9. Zhu Y, Shen R, He J, Wang Y, Han X, Jia Z (2017) China Soil Microbiome Initiative:Progress and Perspective. Bull Chin Acad Sci 32:544–565. http://doi.org/ 10.16418/j.issn.1000-3045.2017.06.002
10. Zheng Y, Sun X, Miao Y, Jiang Y, Huang L (2021) Analysis of the soil microbial community of Cistanche deserticola and Cynomorium songaricum in the saline-alkali soil of Ebinur Lake. Acta Pharm Sinica 56:1178–1187. http:// doi.org/ 10.16438/j.0513-4870.2020-1771
11. Shen L, Xu R, Liu S, Xu CQ, He N, Liu T, Chen J (2016) Characteristics of microbial community structure in rhizosphere soil of Haloxylon ammodendron. Acta Ecol Sin 36:13. https://doi.org/10.5846/stxb201410212063
12. Chaparro JM, Badri, Vivanco JM (2014) Rhizosphere microbiome assemblage is affected by plant development. The ISME journal 2014,8(4): 790–803. https://doi.org/10.1038/ismej.2013.196
13. Sun X, Zhang L, Pei J, Huang LF (2020) Regulatory relationship between quality variation and environment of Cistanche deserticola in three ecotypes based on soil microbiome analysis. Sci Rep 10(1):1–12. https://doi.org/10.1038/s41598-020-63607-2
14. Zhang X, Li X, Rena K, Du NS (2003) RP-HPLC Determination of Echinacoside and Acteoside in Herba CistanchesCultivated on Different Parasitic Species and Habitats. Chin J Pharm Anal volume 23:254–256
15. Zhang GL, Gong ZT (2012) Soil survey laboratory methods.BeiJing, China
16. Liu KP (2017) Evaluation of Uncertainty of Soil Organic Matter Measured by Potassium Dichromate Outside Heating Method. Constr Des Eng 16:101–102. https://doi.org/10.13616/j.cnki.gcjsysj.2017.08.146
17. Edwards AH (1954) The semi-micro Kjeldahl method for the determination of nitrogen. J Appl Chem 4:330–340. https://doi.org/10.1002/jctb.5010040610
18. Cheng J, Ding C, Li X, Zhang T, Wang X (2016) Soil quality evaluation for navel orange production systems in central subtropical China. Soil Tillage Res 155:225–232. https://doi.org/10.1016/j.still.2015.08.015
19. Brookes PC, Landman A, Pruden G, Jenkinson DS (1985) Chloroform fumigation and the release of soil nitrogen: A rapid direct extraction method to measure microbial biomass nitrogen in soil - ScienceDirect. Soil Biol Biochem 17:837–842. https://doi.org/10.1016/0038-0717(85)90144-0
20. Chen J, Liu X, Zheng J, Zhang B, Yu X (2013) Biochar soil amendment increased bacterial but decreased fungal gene abundance with shifts in community structure in a slightly acid rice paddy from Southwest China. Appl Soil Ecol 71:33–44. https://doi.org/10.1016/j.apsoil.2013.05.003
21. Hu B, Liang D, Liu J, Lei L, Yu D (2014) Transformation of heavy metal fractions on soil urease and nitrate reductase activities in copper and selenium co-contaminated soil. Ecotoxicol Environ Saf 110:41–48. https://doi.org/10.1016/j.ecoenv.2014.08.007
22. Jin Y, Liang X, He M, Liu Y, Tian G, Shi J (2016) Manure biochar influence upon soil properties, phosphorus distribution and phosphatase activities: a microcosm incubation study. Chemosphere 142:128–135. https://doi.org/10.1016/j.chemosphere.2015.07.015
23. Abei H (1984) Catalase in vitro. Methods Enzymol 105:121–126. https://doi.org/10.1016/S0076-6879(84)05016-3
24. Schinner F, Öhlinger R, Kandeler E, Margesin R (1996) Enzymes Involved in Nitrogen Metabolism. In: Schinner F, Öhlinger R, Kandeler E, Margesin R (eds) Methods in Soil Biology. Springer, Berlin, Heidelberg. https://doi.org/10.1007/978-3-642-60966-4-11
25. Dennis KL, Wang Y, Blatner NR, Wang S, Saadalla A, Trudeau E, Roers A, Weaver CT, Lee JJ, Gilbert JA et al (2013) Adenomatous polyps are driven by microbe-instigated focal inflammation and are controlled by IL-10–producing T cells. Cancer Res 73:5905–5913. https://doi.org/10.1158/0008-5472.CAN-13-1511
26. Xu N, Tan G, Wang H, Gai X (2016) Effect of biochar additions to soil on nitrogen leaching, microbial biomass and bacterial community structure. Eur J Soil Biology Eur J soil biology 74:1–8. https://doi.org/10.1016/j.ejsobi.2016.02.004
27. Dennis KL, Wang Y, Blatner NR, Wang S, Saadalla A, Trudeau E, Roers A, Weaver CT, Lee JJ, Gilbert JA et al (2013) Adenomatous polyps are driven by microbe-instigated focal inflammation and are controlled by IL-10–producing T cells. Cancer Res 73:5905–5913. https://doi.org/10.1158/0008-5472.CAN-13-1511
28. Zhang H, Wang Y, Chen S, Zhao Z, Feng J, Zhang Z, Lu K, Jia J (2018) Water Bacterial and Fungal Community Compositions Associated with Urban Lakes, Xi'an, China. Environ Res public health 15(3):469. https://doi.org/10.3390/ijerph15030469
29. Chen S, Zhou Y, Chen Y, Gu J (2018) fastp: an ultra-fast all-in-one FASTQ preprocessor. Bioinformatics 34(17):i884–i890. https://doi.org/10.1093/bioinformatics/bty560
30. Magoč T, Salzberg SL (2011) FLASH: fast length adjustment of short reads to improve genome assemblies. Bioinformatics 27:2957–2963. https://doi.org/10.1093/bioinformatics/btr507
31. Stackebrandt E, Goebel BM (1994) Taxonomic Note: A Place for DNA-DNA Reassociation and 16S rRNA Sequence Analysis in the Present Species Definition in Bacteriology. Int J Syst Evol MicroBiol 44:846–849. https://doi.org/10.1099/00207713-44-4-846

32. Edgar RC (2013) UPARSE: highly accurate OTU sequences from microbial amplicon reads. Nat Methods 10:996–998. https://doi.org/10.1038/nmeth.2604
33. Li J, Hu W, Huang X, Xu YP (2018) Investigation of yeast population diversity and dynamics in spontaneous fermentation of Vidal blanc icewine by traditional culture-dependent and high-throughput sequencing methods. Food Res Int 112:66–77. https://doi.org/10.1016/j.foodres.2018.06.011
34. Wang Q, Garrity GM, Tiedje JM, Cole JR (2007) Naïve Bayesian Classifier for Rapid Assignment of rRNA Sequences into the New Bacterial Taxonomy. Appl Environ Microbiol 73(16):5261–5267. https://doi.org/10.1128/AEM.00062-07
35. Schloss PD, Westcott SL, Ryabin T, Hall JR, Hartmann M et al (2009) Introducing mothur: Open-Source, Platform-Independent, Community-Supported Software for Describing and Comparing Microbial Communities. Appl Environ Microbiol 75:7537–7541. https://doi.org/10.1128/AEM.01541-09
36. Chen H, Boutros PC (2011) VennDiagram: a package for the generation of highly-customizable Venn and Euler diagrams in R. BMC Bioinformatics 12(1):1–7. https://doi.org/10.1186/1471-2105-12-35
37. Hong C, Si Y, Xing Y, Li Y (2015) Illumina MiSeq sequencing investigation on the contrasting soil bacterial community structures in different iron mining areas. Environ Sci Pollut Res 22(14):10788–10799. https://doi.org/10.1007/s11356-015-4186-3
38. Banerjee S, Helgason B, Wang L, Winsley T, Belinda, Ferrari BC, Siciliano SD (2016) Legacy effects of soil moisture on microbial community structure and N2O emissions. Soil Biol Biochem 95:40–50. https://doi.org/10.1016/j.soilbio.2015.12.004
39. He Z, Xu M, Deng Y, Kang S, Kellogg L, Wu L et al (2010) Metagenomic analysis reveals a marked divergence in the structure of belowground microbial communities at elevated CO2. Ecol Lett 13:564–575. https://doi.org/10.1111/j.1461-0248.2010.01453.x
40. Hu S, Zhang Y, Shi RJ, Han SQ, Li H, Xu H (2013) Temporal variations of soil microbial biomass and enzyme activities during the secondary succession of primary broadleaved-Pinuskoraiensis forests in Changbai Mountains of Northeast China. Chin J Appl Ecol 24:366. http://doi.org/10.1899/04-106.1
41. Silva-Olaya AM, Mora-Motta DA, Cherubin MR, Grados D et al (2021) Soil enzyme responses to land use change in the tropical rainforest of the Colombian Amazon region. PLoS ONE 16:e0255669. http//doi.org/10.1371/journal.pone.0255669
42. Liu Q, Wang S, Li K, Qiao J, Guo Y, Liu Z, Guo X (2021) Responses of soil bacterial and fungal communities to the long-term monoculture of grapevine. Appl Microbiol Biotechnol 105:7035–7050. http//doi.org/doi: 10.1007/s00253-021-11542-1
43. Zhao J, Xie HJ, Zhang J (2020) Microbial Diversity and Physicochemical Properties of Rhizosphere Microenvironment in Saline-alkali Soils of the Yellow River Delta. Huanjing Kexue 41:1449–1455. http//doi.org/10.13227/j.hjkx.201908044
44. Zhang D, Meng KX, Hao YF, Yu, Han HY et al (2016) Comparative proteomic analysis of cucumber roots infected by Fusarium oxysporum f. sp. cucumerium Owen. Physiol Mol Plant Pathol 96:77–84. https://doi.org/10.1016/j.pmpp.2016.09.002
45. Schnürer J, Clarholm M, Rosswall T (1985) Microbial biomass and activity in an agricultural soil with different organic matter contents. Soil Biol Biochem 17:611–618. https://doi.org/10.1016/0038-0717(85)90036-7
46. Vries FTD, Hoffland E, Eekeren NV, Brussaard L, Bloem J (2006) Fungal/bacterial ratios in grasslands with contrasting nitrogen management. Soil Biol Biochem 38:2092–2103. https://doi.org/10.1016/j.soilbio.2006.01.008
47. Hong Y, Zhao D, Zhang F, Shen G, Yuan Y, Gao Y, Yan L, Wei D, Wang W (2021) Soil water-stable aggregates and microbial community under long-term tillage in black soil of Northern China. Ecotoxicology 30:1754–1768. http://doi.org/ 10.1007/s10646-020-02317-x
48. Cusack DF, Silver WL, Torn MS, Burton SD, Firestone MK (2011) Changes in microbial community characteristics and soil organic matter with nitrogen additions in two tropical forests. Ecology 92:621–632. https://doi.org/10.1890/10-0459.1
49. Nemergut DR, Townsend AR, Sattin SR, Freeman KR et al (2008) The effects of chronic nitrogen fertilization on alpine tundra soil microbial communities: implications for carbon and nitrogen cycling. Environ Microbiol 10:3093–3105. https://doi.org/10.1111/j.1462-2920.2008.01735.x
50. Moore JAM, Anthony MA, Pec GJ, Trocha LK et al (2021) Fungal community structure and function shifts with atmospheric nitrogen deposition. Glob Change Biol 27:1349–1364. http://doi.org/10.1111/gcb.15444
51. Gu YF, Zhang XP, Tu SH, Lindstrrom K (2009) Soil microbial biomass, crop yields, and bacterial community structure as affected by long-term fertilizer treatments under wheat-rice cropping. Eur J Soil Biol 45:239–246. https://doi.org/10.1016/j.ejsobi.2009.02.005
52. Yang T, Adams JM, Shi Y, He JS, Jing X et al (2017) Soil fungal diversity in natural grasslands of the Tibetan Plateau: associations with plant diversity and productivity. New Phytol 215(2):756–765. https://doi.org/10.1111/nph.14606
53. Shi X, Zhao X, Ren J, Dong J, Zhang H et al (2021) Influence of Peanut, Sorghum, and Soil Salinity on Microbial Community Composition in Interspecific Interaction Zone. Front Microbiol 12:1306. https://doi.org/10.3389/fmicb.2021.678250
54. Liu M, Abdel-Mageed WM, Ren B, He W, Huang P et al (2014) Endophytic Streptomyces sp. Y3111 from traditional Chinese medicine produced antitubercular pluramycins. Appl Microbiol Biotechnol 98:1077–1085. https://doi.org/10.1007/s00253-013-5335-6
55. Yelle DJ, Ralph J, Lu F, Hammel KE (2008) Evidence for cleavage of lignin by a brown rot basidiomycete. Environ Microbiol 10(7):1844–1849. https://doi.org/10.1111/j.1462-2920.2008.01605.x
56. Yang LB, Sui X, Wei D, Cui FX, Zhu DG, Ni HW (2019) Fungal diversity in the brown coniferous forest soils of Daxing'anling Mountains, Northeast China. J Appl Ecol 30:3411–3418. http://doi.org/ 10.13287/j.1001-9332.201910.030
57. Gao WW, Kang Y, Hong L, Wang QY (2016) Basic soil physicochemical properties and soil fungal diversity under different forest types of urban forest. J Northeast Forestry Univ 44:89–94. https://doi.org/10.13759/j.cnki.dlxb.2016.03.002
58. Wu GY, Cheng FS, Wan SZ, Liu R, Yang D, HU TY, Zhang Y (2019b) Phosphate Solubilizing Characteristics and Growth Promoting Effect of Aspergillus neoniger on Phyllostachys edulis Seedling. For Res 32:144–145. http://doi:10.13275/j.cnki.lykxyj.2019.04.019
59. Komai Si, Hosoe T, Itabashi T et al (2006) New penicillide derivatives isolated from Penicillium simplicissimum. J Nat Med 60:185–190. https://doi.org/10.1007/s11418-005-0028-9

Figures

Figure 1

(a), (b), and (c) are *Cistanche salsa* of different host plants. (a) is *Ceratoides*, (b) is *Anabasis*, (c) is *Atriplex*.

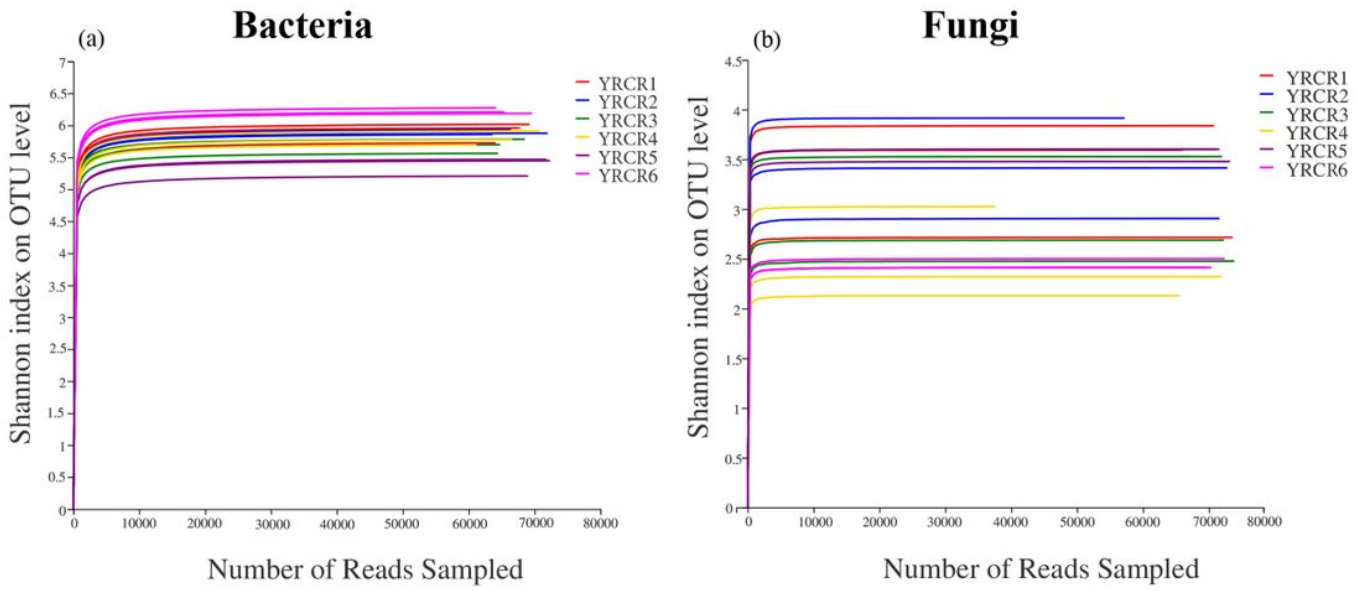

Figure 2

Rarefaction curves of OTUs were clustered for a dissimilarity threshold of 3%. (a) represents the rarefaction curves of the bacteria. (b) represents the rarefaction curves of the fungal.

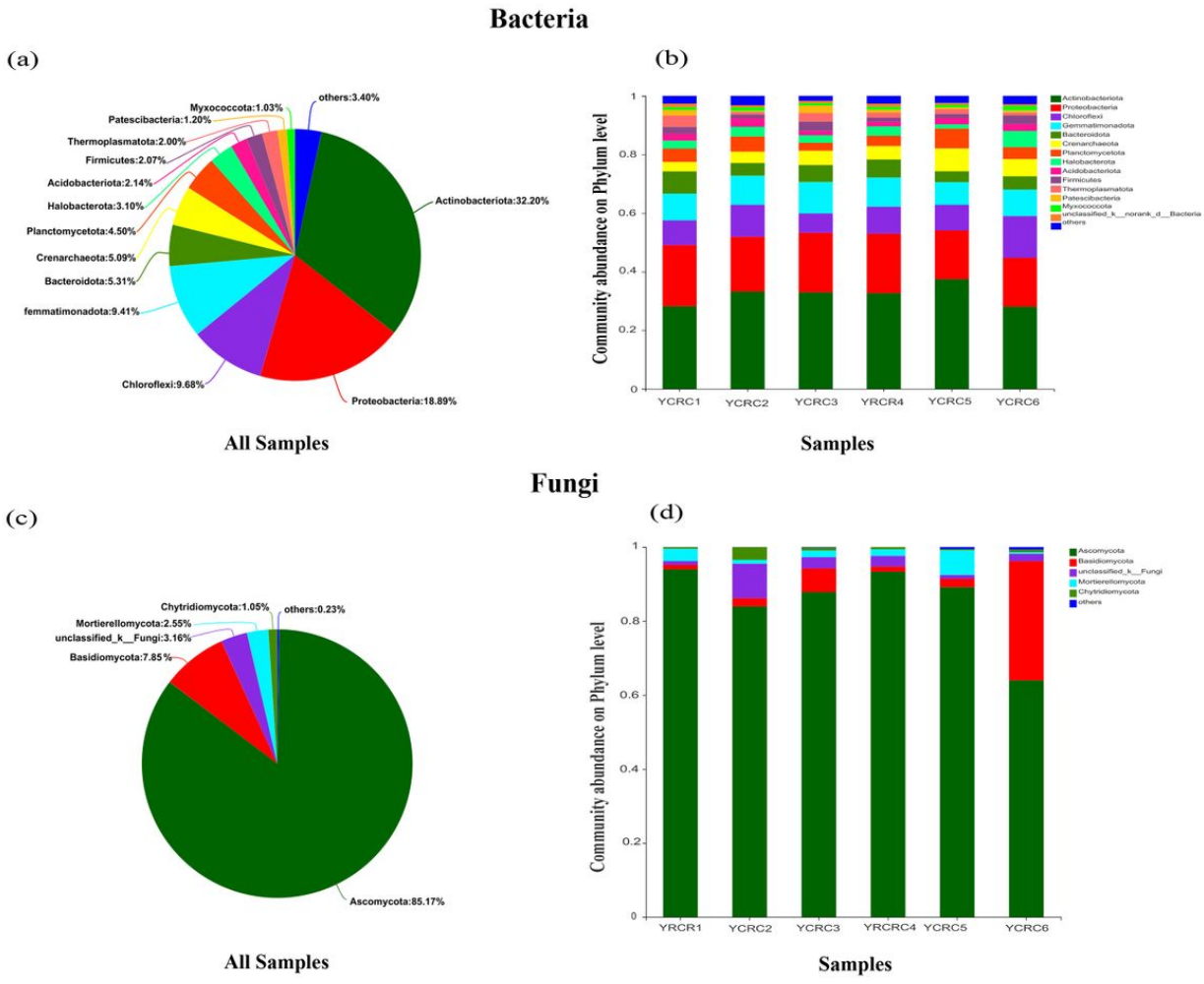

Figure 3

(a) is the bacterial community analysis pieplot on phylum level of all samples; (b) is the relative abundance of bacterial on phylum level. (c) is community abundance of fungal in all samples on phylum level; (d) is community abundance of fungal in each sample on phylum level.

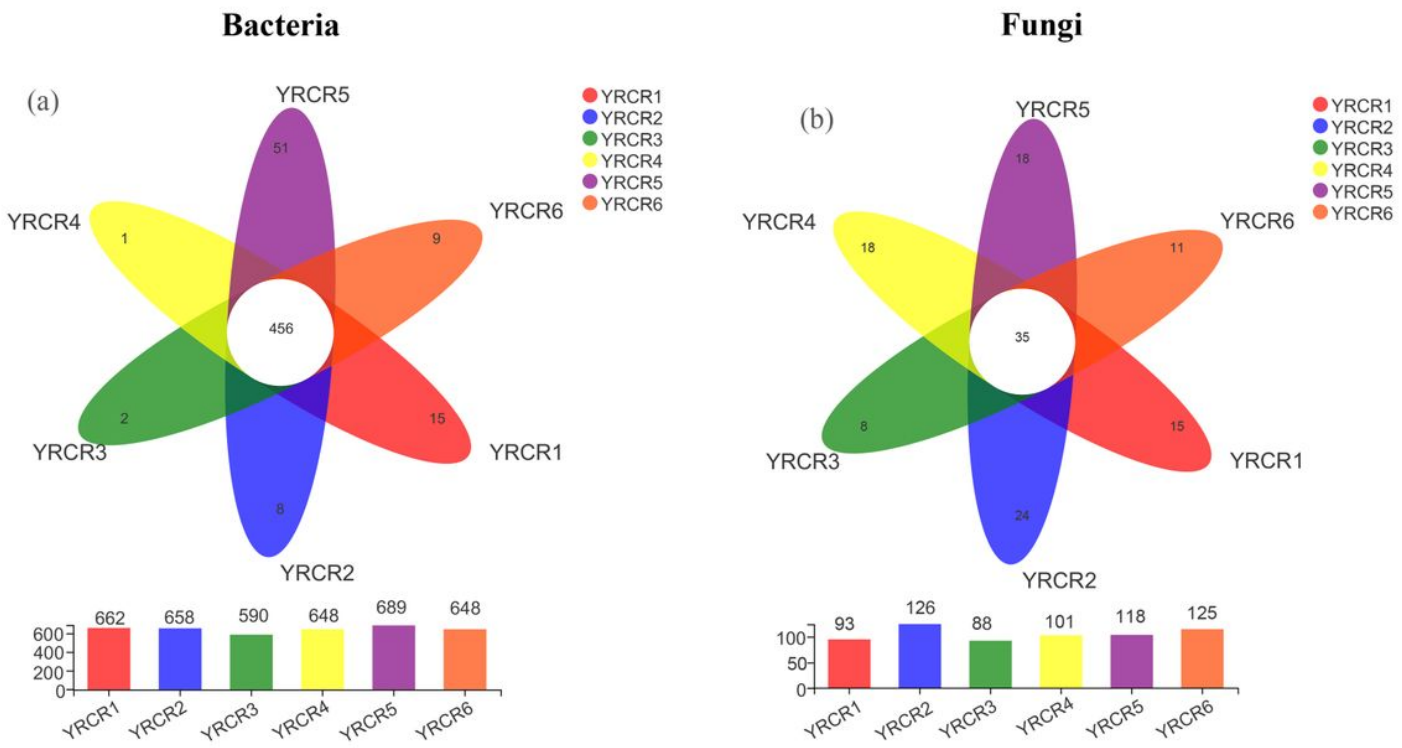

Figure 4

Veen diagram at the genus level of six samples. (a) represents bacteria, (b)represents gungal.Each circle with different colors in the diagram represents a group; middle core numbers represent the number of genus common to all groups.

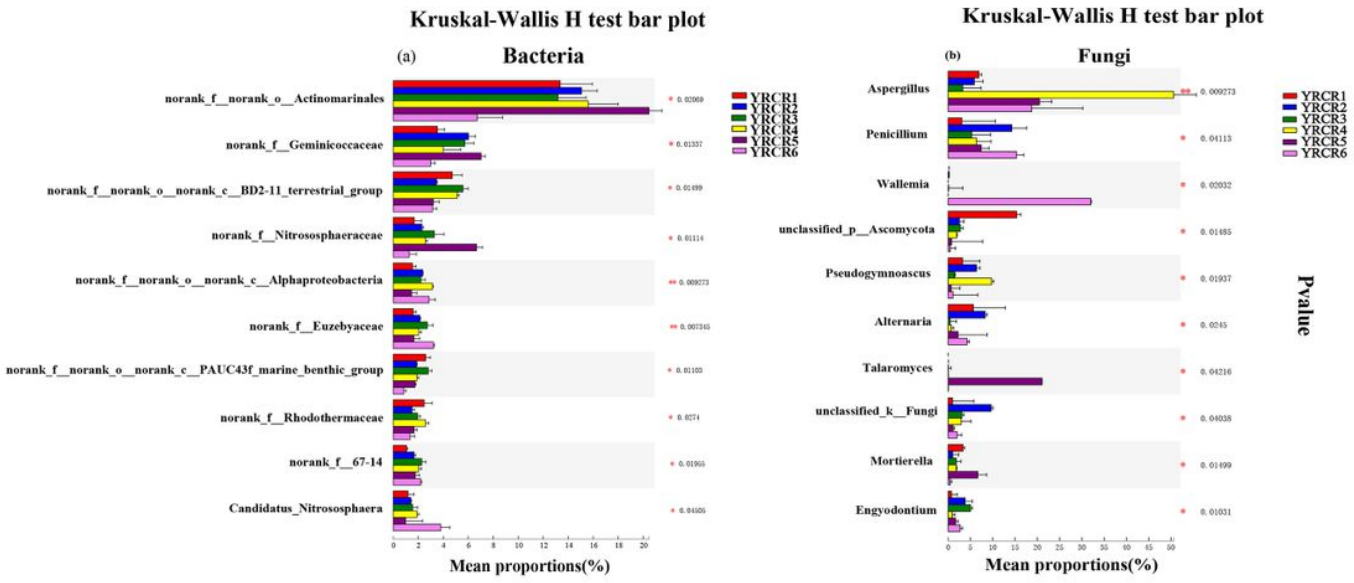

Figure 5

Species difference analysis of all samples on genus level. The y-axis represents the genus levels of species, and the x-axis represents the percentage of species average relative abundance in each sample group. (a) is represent bacteria; (b) is represent Fungi. The Kruskal-Wallis rank-sum test was used to show significant differences (*: 0.01 < P < = 0.05, **: 0.001 < P < = 0.01).

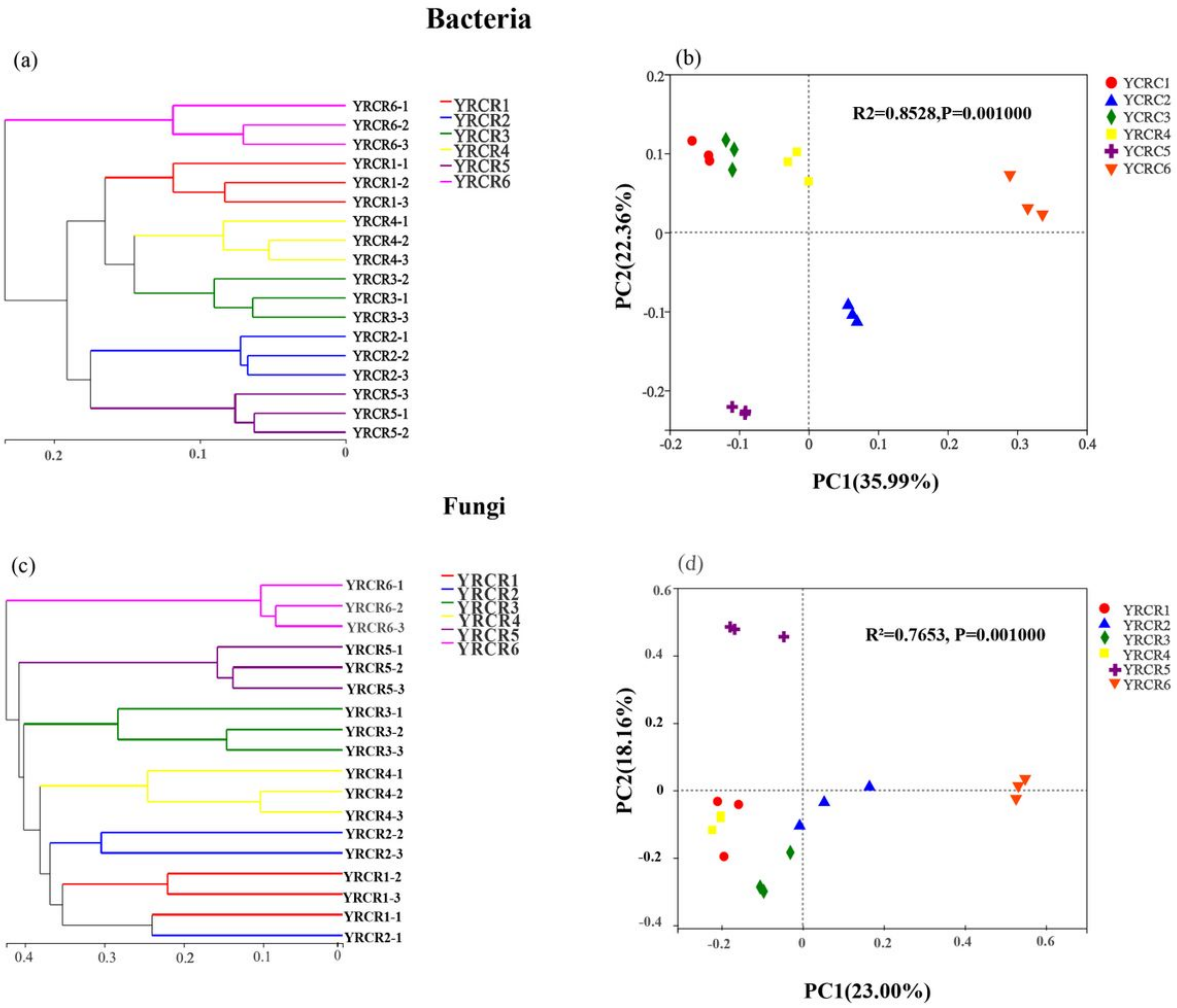

Figure 6

(a) is Hierarchical clustering tree of bacterial on OTU level. (b) is principal coordinate analysis (PCoA) of the bacterial diversity. (c) is Hierarchical clustering tree of fungal on OTU level. (d) is principal coordinate analysis (PCoA) of the fungal diversity. The hierarchical clustering and PCoA plots were using Bary-Curtis distance method at OUT level.

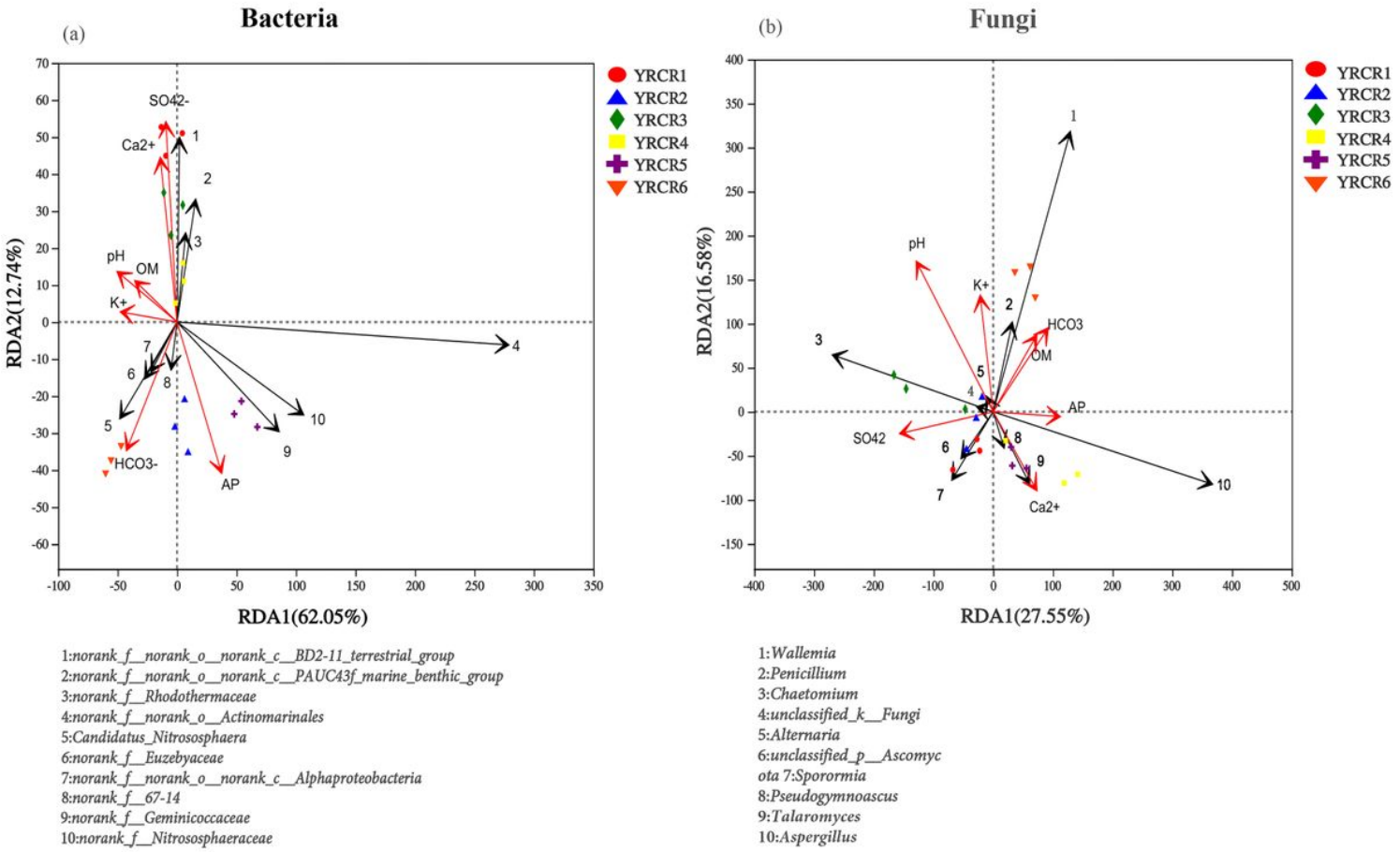

Figure 7

(a) is RDA of the correlation between bacterial and soil physicochemical on genus level. (b) is RDA of the correlation between fungal and soil physicochemical.

Supplementary Files

This is a list of supplementary files associated with this preprint. Click to download.

- FigureS1.jpg
- FigureS2.jpg
- TableSI.docx